Electronic Supplementary Material

Engineering hyaluronic acid-based nanoassemblies for monoclonal antibody delivery – design, characterization, and biological insights

Ana M. López-Estévez[1,2,3], Y. Zhang[4], María Medel[5], Iker Arriaga[6], Lucía Sanjurjo[3], Cristian Huck-Iriart[7], Nicola G.A. Abrescia[6,8], María J. Vicent[5], Defang Ouyang[4], Dolores Torres[2], and María José Alonso[1,2,3] (✉)

[1] *Center for Research in Molecular Medicine and Chronic Diseases (CiMUS), University of Santiago de Compostela, Santiago de Compostela 15782, Spain*
[2] *Department of Pharmacology, Pharmacy and Pharmaceutical Technology, School of Pharmacy, University of Santiago de Compostela, Santiago de Compostela 15782, Spain*
[3] *Health Research Institute of Santiago de Compostela (IDIS), Santiago de Compostela 15782, Spain*
[4] *State Key Laboratory of Quality Research in Chinese Medicine, Institute of Chinese Medical Sciences (ICMS), University of Macau, Macau 999078, China*
[5] *Polymer Therapeutics Laboratory and CIBERONC Prince Felipe Research Centre, Valencia E-46012, Spain*
[6] *Structure and Cell Biology of Viruses Lab, CIC bioGUNE, Basque Research and Technology Alliance (BRTA), Derio 48160, Spain*
[7] *ALBA Synchrotron Light Source, Experiments Division, Cerdanyola del Vallès, Barcelona 08290, Spain*
[8] *IKERBASQUE, Basque Foundation for Science, Bilbao 48009, Spain*

Supporting information to https://doi.org/10.1007/s12274-024-6826-8

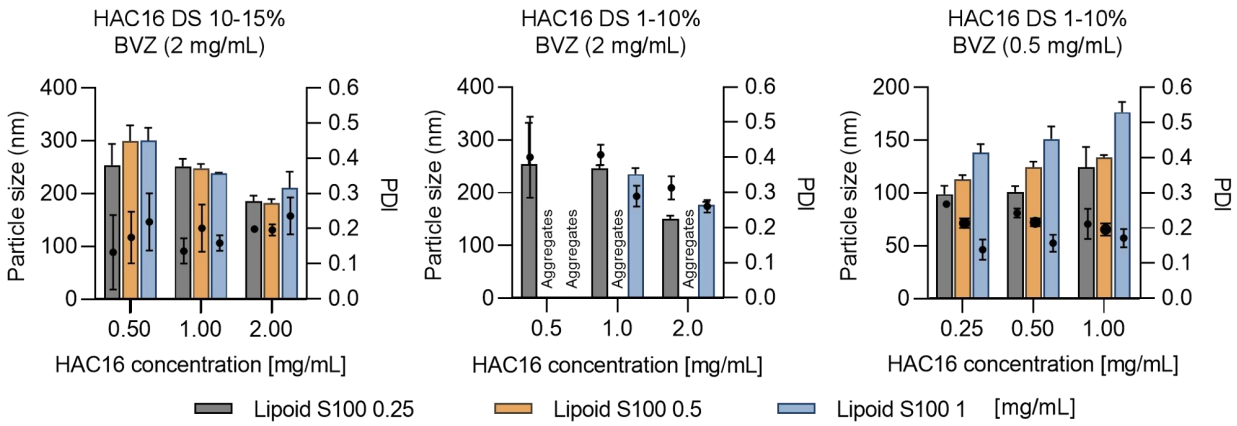

Figure S1 Screening of different concentrations of HAC16 30–70 kDa and Lipoid S100. HAC16 polymer with two amounts of hydrophilic chains per polymer: DS 10%–15% and DS 1%–10% were tested. The final concentration of BVZ was fixed in 2 and 0.5 mg/mL. Bars: particle size, PDI: dots. The physicochemical properties were determined by dynamic light scattering (particle size and PDI) and laser Doppler anemometry (Zeta potential). Data are represented as mean ± SD, $n = 3$.

Address correspondence to mariaj.alonso@usc.es

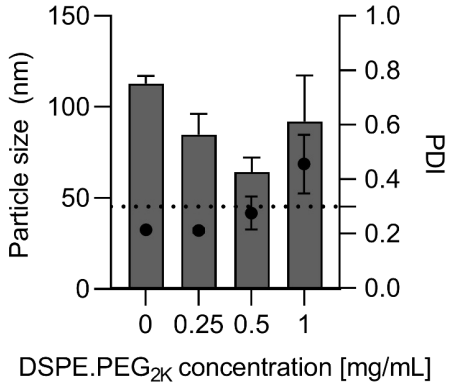

Figure S2 Physicochemical properties of resulting prototypes. Screening of different concentrations of DSPE.PEG_{2K} over prototype HA-100. The final concentration of BVZ was fixed in 0.5 mg/mL. Bars: particle size, PDI: dots. The physicochemical properties were determined by dynamic light scattering (particle size and PDI) and laser Doppler anemometry (Zeta potential). Data are represented as mean ± SD, $n \geq 3$.

Table S1 DLS mean particle size and NTA distribution parameters (mean, mode and D10/50/90) of BVZ-loaded HANAs

Proto-type	DLS	Nanoparticle tracking analysis (NTA)					
	Physicochemical properties						Concentration (particles/mL)
	Mean	Mean	Mode	D10	D50	D90	
HA-200	195.4 ± 14	132.9 ± 18**	86.7 ± 66	86.5 ± 11	124.3 ± 14	187.9 ± 36	$3.9 \times 10^{12} \pm 7.2 \times 10^{11}$
HA-160	161.8 ± 17	144.3 ± 13	130.0 ± 20	83.5 ± 7	137.3 ± 14	214.7 ± 20	$3.3 \times 10^{12} \pm 1.1 \times 10^{12}$
HA-100	107.5 ± 14	150.9 ± 55*	119.1 ± 38	80 ± 23	134.4 ± 44	240 ± 105	$2.4 \times 10^{11} \pm 1.2 \times 10^{11}$
PEGHA-100	78.9 ± 8	138.7 ± 9	98.2 ± 7	74 ± 18	123.6 ± 5	220 ± 24	$2.4 \times 10^{11} \pm 6.6 \times 10^{10}$

Statistical analysis was done following an unpaired t-test but HA-100 (Mann-Whitney test) between mean particle sizes (*$P < 0.05$; **$P < 0.01$).

Data are expressed as mean ± SD, $n \geq 3$.

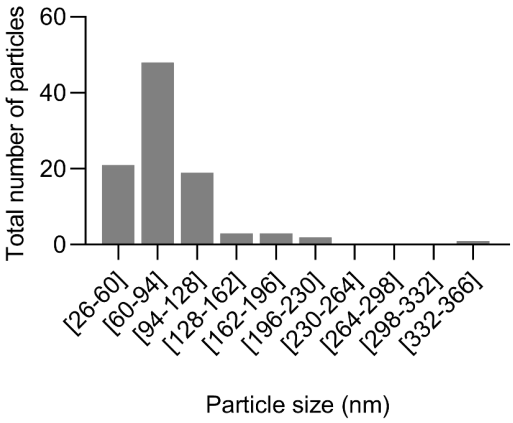

Figure S3 Cryo-TEM histogram based on diameter size of PEGHA-100. Total number of particles: n = 101. Note that the smallest ones, below 25 nm, have been discarded for the count.

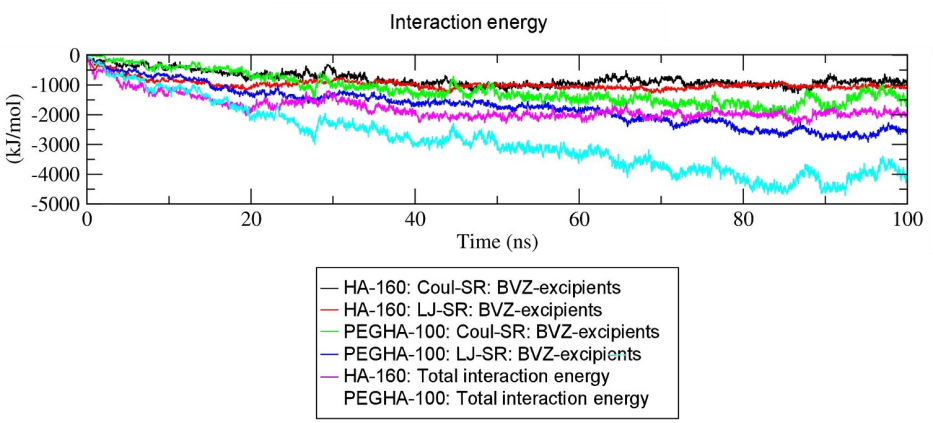

Figure S4 Interaction energy (Coul-SR: Coulomb interaction, LJ-SR: van der Waals interaction, unit: kJ/mol) between the antibody and the remaining molecules during 100 ns MD simulation.

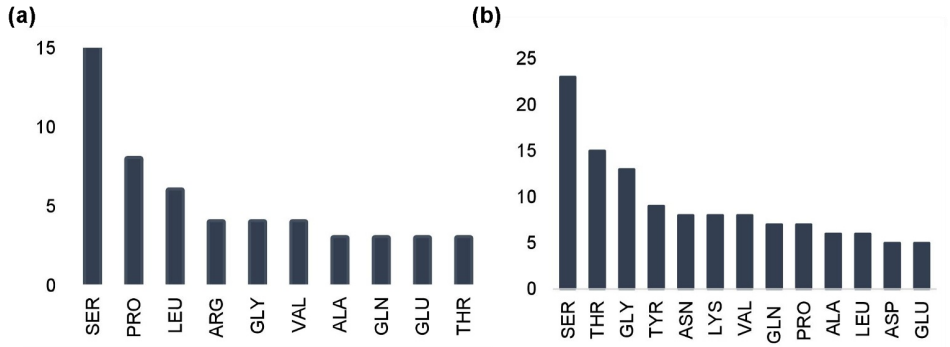

Figure S5 Contacted amino residues among existing components in HA-160 (a) and PEGHA-100 (b). Those contacted aa below 3 and 5, respectively, were discarded.

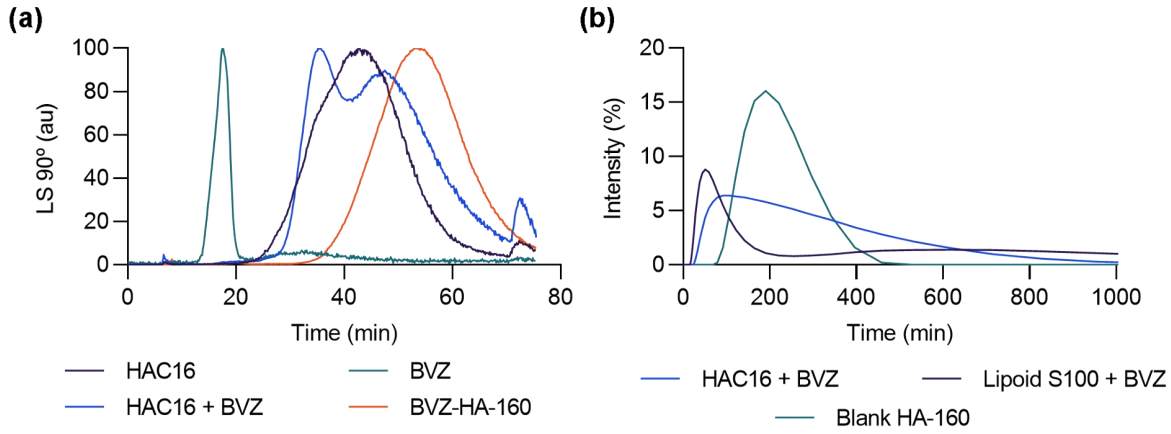

Figure S6 Interaction profile of the components of the HA-160 and the BVZ. (a) AF4 fractograms of HA-160 with a light scattering 90° detector. (b) Intensity histograms based on particle size distribution by DLS.

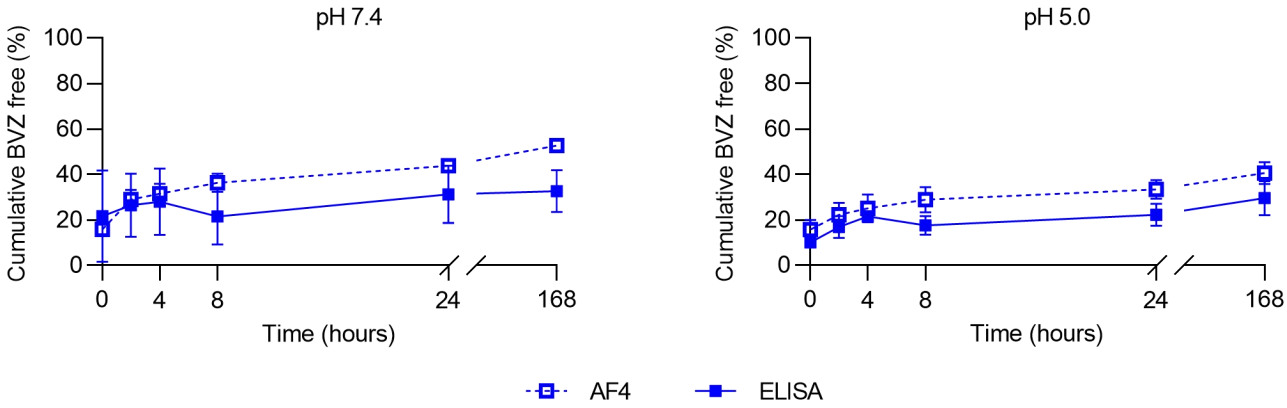

Figure S7 Release profile of HA-160 upon incubation in PBS pH 7.4 and 5.0 at 37 ºC. The cumulative amount of free BVZ was quantified by ELISA (filled squares) and AF4 with UV and RI detectors (empty squares). Data are represented as mean ± SD, $n = 3$.

Table S2 Summary of the most relevant nanocarriers for the entrapment of bevacizumab in cancer therapy, including the HANAs technology

BVZ-loaded nanocarrier (drug co-loaded) **Co-administered therapy**	**Physicochemical properties (particle size, PDI)** **AE (quantification method), LC** **Release profile** **Stability in storage conditions**	**Cytoto-xicity / uptake studies?**	**Superior *in vivo* efficacy of the NP vs free BVZ?** **Superior *in vivo* efficacy in combination?**	**Ref.**
HANAs	Particle size 79–196 nm; PDI 0.23–0.25 AE 67%–99 % (ELISA); LC 22%–47% Release: burst release about 20%, followed by a 20%–60% up to 168 hours. Stability in suspension at 4 ºC Storage conditions following ICH guidelines	Yes / Yes	-	-
PEG-HSA NPs	Particle size 301 nm; PDI 0.13 AE 92% (ELISA); LC 145 µg/mg Release: burst release about 20%, followed by a 60% up to 24 hours.	No	No / -	[1]
Lipid-polymer hybrid NPs (erlotinib)	Particle size 103–121 nm; PDI 0.11–0.15 AE 84%–85% (UV spectroscopy); LC 5.3%–7.8% Release: 80% release after 72 hours, with differences at pH 7.4 and 6.0 Stability in suspension at 4 ºC	Yes / Yes	Yes (tumor volume) / Yes	[2]

Liposomes Doxorubicin-loaded HER2 Ab decorated liposomes	Particle size: 152 nm AE 37% (ELISA) Release: burst release about 21%, followed by a 55% up to 48 hours.	No / Yes	No control with free BVZ / Yes	[3]
Liposomes (Benzoporphyrin derivative)	Particle size 120 nm; PDI 0.1 AE 60%–80% Release 85% after 72 hours Stability in suspension at 4 ºC	Yes / Yes	No / Yes	[4]
PLGA-NPs	Particle size 199 nm; PDI 0.16 AE 83% (HPLC); LC 1.62% Release 14% after 168 hours at pH 6 and lower at pH 7.4 Stability in suspension at 4 ºC Storage conditions following ICH guidelines	Yes / Yes	No (tumor volume) Yes (vascularization)	[5–8]
Chitosan NPs	Particle size 137–283 nm; PDI 0.24–0.3 AE 37%–75% (UV spectroscopy) Release 62%–74% after 48 hours.	Yes / No	Yes (angioge-nesis) / -	[9]
CD44v6 Fab-PEG PLGA NPs	Particle size 184–346 nm; PDI 0.35–0.39 AE 87% (HPLC); LC 7.9%	Yes / Yes	-	[10]
Tween 80/Tween 20/Brij 97 NPs	Particle size 239–774 nm PDI 0.1–0.2	Yes / Yes	-	[11]

mAb monoclonal antibody; HANAs hyaluronic-acid based nanoassemblies; NPs nanoparticles; PDI polydispersity index; AE association efficiency; LC loading capacity; PLGA poly(lactic-co- glycolic) acid; PEG polyethylene glycol; HSA human serum albumin; ELISA enzyme-linked immunosorbent assay; HPLC high-performance liquid chromatography

Table S3 Physicochemical properties of DiD-labeled blank and BVZ-loaded prototypes HA-160 and PEGHA-100

Prototype	Physicochemical properties		
	Particle size (nm)	PDI	Zeta potential (mV)
HA-160 (blank)	174 ± 9	0.20	−15 ± 2
HA-160 (BVZ)	158 ± 16	0.17	−13 ± 2
PEGHA-100 (blank)	80 ± 5	0.23	−13 ± 1
PEGHA-100 (BVZ)	75 ± 10	0.14	−13 ± 0.1

DiD final concentration is 10 and 0.01 ppm, respectively. The physicochemical properties were determined by dynamic light scattering (particle size and PDI) and laser Doppler anemometry (Zeta potential). Data are expressed as mean ± SD, $n \geq 3$, except for Zeta potential of PEGHA-100 (BVZ): $n = 2$.

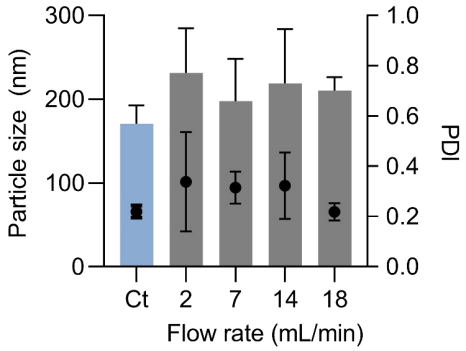

Figure S8 Physicochemical characteristics of HA-160 when prepared by microfluidics technique at different flow rates and compared with the standard pipette injection (C_t). Feed ratio HAC16/BVZ: Lipoid S100 (12.5:1) and (4:1). The physicochemical properties were determined by dynamic light scattering (particle size and PDI) and laser Doppler anemometry (Zeta potential). Bars: particle size, PDI: dots. Data are expressed as mean ± SD, $n \geq 3$.

References:

[1] Luis de Redín I, Expósito F, Agüeros M, Collantes M, Peñuelas I, Allemandi D, Llabot JM, Calvo A, Irache JM. In vivo efficacy of bevacizumab-loaded albumin nanoparticles in the treatment of colorectal cancer. *Drug Deliv Transl Res*. **2020**, *10*, 635-645.

[2] Pang J, Xing H, Sun Y, Feng S, Wang S. Non-small cell lung cancer combination therapy: Hyaluronic acid modified, epidermal growth factor receptor targeted, pH sensitive lipid-polymer hybrid nanoparticles for the delivery of erlotinib plus bevacizumab. *Biomedicine & Pharmacotherapy.* **2020**, *125*, 109861.

[3] Tang Y, Soroush F, Tong Z, Kiani M, Wang B. Targeted multidrug delivery system to overcome chemoresistance in breast cancer. *Int J Nanomedicine*. **2017**, *12*, 671–681.

[4] Tangutoori S, Spring BQ, Mai Z, Palanisami A, Mensah LB, Hasan T. Simultaneous delivery of cytotoxic and biologic therapeutics using nanophotoactivatable liposomes enhances treatment efficacy in a mouse model of pancreatic cancer. *Nanomedicine*. **2016**, *12*, 223–234.

[5] Sousa F, Costa-Pereira AI, Cruz A, Ferreira FJ, Gouveia M, Bessa J, Sarmento B, Travasso RDM, Mendes Pinto IS. Intratumoral VEGF nanotrapper reduces gliobastoma vascularization and tumor cell mass. Journal of Controlled Release. **2021**, 339, 381-390.

[6] Sousa F, Cruz A, Pinto IM, Sarmento B. Nanoparticles provide long-term stability of bevacizumab preserving its antiangiogenic activity. *Acta Biomater.* **2018**, *78*, 285-295.

[7] Sousa F, Dhaliwal HK, Gattacceca F, Sarmento B, Amiji MM. Enhanced anti-angiogenic effects of bevacizumab in glioblastoma treatment upon intranasal administration in polymeric nanoparticles. *Journal of Controlled Release.* **2019**, *309*, 37–47.

[8] Sousa F, Cruz A, Fonte P, Pinto IM, Neves-Petersen MT, Sarmento B. A new paradigm for antiangiogenic therapy through controlled release of bevacizumab from PLGA nanoparticles. *Sci Rep.* **2017**, 7, 3736.

[9] Abdi , Arkan E, Eidizadeh M, Valipour E, Naseriyeh T, Gamizgy YH, Mansouri K. The possibility of angiogenesis inhibition in cutaneous melanoma by bevacizumab-loaded lipid-chitosan nanoparticles. *Drug Deliv Transl Res.* **2023**, 13, 568-579.

[10] Baião A, Sousa F, Oliveira AV, Oliveira C, Sarmento B. Effective intracellular delivery of bevacizumab via PEGylated polymeric nanoparticles targeting the CD44v6 receptor in colon cancer cells. *Biomater Sci*. **2020**, *8*, 3720–3729.

[11] Srinivasan AR, Lakshmikuttyamma A, Shoyele SA. Investigation of the Stability and Cellular Uptake of Self-Associated Monoclonal Antibody (MAb) Nanoparticles by Non-Small Lung Cancer Cells. *Mol Pharm*. **2013**, *10*, 3275–3284.